Václav Petříček*, Lukáš Palatinus, Jakub Plášil and Michal Dušek

JANA2020 – a new version of the crystallographic computing system JANA

https://doi.org/10.1515/zkri-2023-0005
Received February 7, 2023; accepted April 13, 2023;
published online April 27, 2023

Abstract: We present the crystallographic program JANA2020, the successor of JANA2006. JANA2020 has new, technically different graphics and structure plot-driven intuitive control. Tools known from JANA2006 were revised and inserted into a new logical scheme, and their control connected with the structure plot. Some of the tools were considerably improved. We focus on the details of the most dynamically developing parts, namely twinned structures, magnetic structures, and structure analysis based on electron diffraction data.

Keywords: crystallographic computing; magnetic structures; modulated structures; solution and refinement structures; twinning.

1 Introduction

JANA originated in 1984 at the university in Buffalo, USA, where Václav Petříček worked at the group of the late Prof. Phillip Coppens. Phillip readily recognised the importance of modulated structures for the research on conductivity and superconductivity and needed analytical software for such a class of compounds. Václav had experience programming SDS, an unpublished Structure Determination Software for standard structures. During his stay in Buffalo, he created the first version of JANA – a refinement program for modulated structures.

In the following years, JANA grew into a widely applicable crystallographic system covering standard, modulated, and magnetic structures refined against X-ray, neutron, and electron diffraction data from single crystals, powders, and nanocrystals. These capabilities were included in the well-known program version JANA2006 [1], used by several thousand users and cited about 500 times yearly.

The goal of JANA2006 was to develop a crystallographic tool for solving exceptionally complicated structures and offer such a possibility to a broad crystallographic community. Therefore, simplicity and graphical user tools have always been the priority, and JANA2006 has been considered a reasonably user-friendly tool for a long time. However, the bar for the graphical interface was set higher by new crystallographic tools like OLEX2 [2], and the homemade graphics of JANA2006, although very convenient for non-standard graphical tools, could not compete anymore in terms of speed and clarity. Especially the fact that JANA2006 did not include a built-in structure viewer and editor was rather inconvenient and limiting.

JANA2020 was developed with the motivation to overcome these limitations. It has modern and fast graphics based on the Winteracter library [3]. The new interface allowed for rearranging and optimising tools known from JANA2006 and connecting the tools with a new plotting program, JANADRAW. In addition, JANA2020 offers extended support for twins and magnetic structures and many other improvements stemming from the continuous development of the underlying crystallographic methods. The new graphical interface and some of the most important developments are described hereafter.

2 Basic features

JANA2020 comprises the whole cycle from structure solution, completing and refining the structure model to interpretation and publishing tools. It is based on extended and revised tools of JANA2006. Here we briefly summarise the basic features of JANA2020, which are shared with JANA2006 and are described in more detail in Ref. [1]. The tools and methods considerably improved compared with JANA2006 are presented in the following chapters.

JANA2020 works with standard (*i.e.*, non-modulated) and modulated structures up to three modulation vectors. It deals with nuclear or magnetic structures, and the modulation can be commensurate or incommensurate. Furthermore, nuclear and magnetic structures can be combined in the same refinement and can be a twin or multiphase. As a

***Corresponding author: Václav Petříček**, Institute of Physics, Academy of Sciences of the Czech Republic, v.v.i., Na Slovance 2, 182 00 Praha 8, Czech Republic, E-mail: petricek@fzu.cz
Lukáš Palatinus, Jakub Plášil and Michal Dušek, Institute of Physics, Academy of Sciences of the Czech Republic, v.v.i., Na Slovance 2, 182 00 Praha 8, Czech Republic

particular class of materials, Jana2020 also supports composite structures [4].

Input diffraction data of single crystals or powders are accepted from X-ray and neutron sources, including TOF data. Various kinds of data can be combined and used for the same structure model. Electron diffraction data are also supported, and a special type of refinement against electron diffraction data, called dynamical refinement, is available, as explained in a dedicated chapter.

The built-in tool for structure solution is Superflip [5], which provides *ab-initio* structure models for standard and modulated structures. Other structure solution programs like Shelxt [6] and Sirware [7] can also be linked to Jana2020 and used directly from the interface. Jana2020 also contains random procedures for finding by trials and errors q-vector in a powder structure and initial parameters of modulation functions.

Symmetry can be determined by the classical tools based on systematic absences and included in the symmetry wizard, or it can be determined using the possibilities of the structure solution software. A combination of both approaches, nevertheless, is recommended. The symmetry wizard of Jana2020 takes into account various possibilities of twinning and its impact on merging symmetry-equivalent reflections, including reticular twinning following from the existence of a supercell of higher symmetry. Symmetry wizard can also be applied to modulated structures. Jana2020 can connect to Stokes & Campbell SSG test for advanced symmetry analysis [8].

The refinement procedure of Jana2020 (see Ref. [1] for technical details) can determine the parameters of individual atoms or rigid bodies. In both cases, refinement can include modulated occupancy, position, or displacement parameters described by harmonic or crenel [9] modulation functions. For individual atoms, atomic displacement parameters (ADP) can be described using the Gram-Charlier expansion up to the sixth order [10], which helps describe disorder or the delocalised electron density of ionic conductors [11]. Jana2020 also includes multipole refinement based on the Hansen-Coppens formalism [12]. Refinement can work with an arbitrary number of twin or multiphase domains, and – when needed - the structure model can be refined from data combined from various diffraction sources, e.g., neutron and X-ray data or X-ray data acquired with several wavelengths. Jana2020 also refines powder profile parameters for powder data, including various functions for profile asymmetry and the fundamental profile parameters [13]. Except for profile parameters, the program automatically refines all parameters allowed by symmetry and not fixed by user-defined commands.

Parameters of the structure model can be connected using a rich palette of constraints, restraints and user equations where each structure parameter can be used with its unique identifier. Moreover, individual atoms can be bound by user-defined local symmetry operations not included in the structure model's space group. A typical application of the local symmetry operations is comparing higher and lower symmetry of structure models. Still, the concept can also be used to introduce non-crystallographic symmetry of molecules (e.g., C60, [14]) and to model exceptional disorder cases.

The changes in the structure model during refinement are immediately reflected in the plotting program JanaDraw, which can also display the peak positions from the difference Fourier map. The Contour tool is used for a more detailed analysis of electron density, which is particularly important for modulated structures, where the program automatically generates de Wolff sections through a multidimensional Fourier map. The program can also visualise sections defined by atoms chosen by the user in JanaDraw. Jana2020 calls Mce [15] or Vesta [16] for the isosurface representation of electron density. The geometry parameters of the resulting structure model are calculated by the Dist tool or – for modulated structures – visualised by the Grapht tool as a function of the internal coordinate *t*. For anharmonic ADP refined with higher-order tensors, results are plotted as probability density function (p.d.f.) or joint probability density function (j.p.d.f.) maps. For print-quality figures needed for publication, Jana2020 can link external plotting programs like Diamond [17], Vesta [16] or Mercury [18]. The structure analysis results are exported as a CIF file based on the core CIF, pdCIF, magCIF and msCIF dictionaries [19].

Transformation tools belong to the most elaborated part of Jana2020. They are used in all steps of structure analysis, e.g., group-subgroup transformation, unit cell transformations, the transformation from the centered to the primitive unit cell and *vice versa*, origin shift, change of enantiomorph, change of modulation vector, the transformation of a commensurate structure to the supercell or a modulated structure to the average structure.

2.1 User interface

The program layout is provided in Figure 1. Each structure has its project name connecting all files related to the structure model. The Main menu is used for tasks changing the project (e.g., creating a new structure or transforming a structure model to a subgroup) and tasks independent of the project (e.g., Settings and Tools). Focus buttons define

the main point of interest, the structure plot created by the JANADRAW tool, or the powder profile plot created by the Powder profile viewer. The plot of the crystal structure and powder profile reflects in real-time all changes due to user settings or structure/profile refinement. The Command tree contains all tools related to the given project, and the most frequently used ones have a corresponding Quick button.

Our goal was to develop an entirely intuitive interface for simple tasks and helpful support for complex tasks without compromising the possibilities of the program. Thus, each tool known from JANA2006 still has its original (or improved) manual interface for detailed setup, but – whenever possible – the tools are also connected with the structure plot for graphical control.

For example, the structure parameters of atoms can be edited by selecting them in the JANADRAW plot followed by a right-click. Still, the same can be done by opening "Edit structure parameters" → "Edit atoms" in the Command tree. The second way is helpful for large structures where the structure plot does not provide an easy survey or when the selection is more quickly made with wildcards. Finally, the graphical mode significantly improves the definition of the sections through Fourier maps by selecting atoms defining the section plane by mouse, or setting up rigid body positions by showing the target positions in the plot. Adding access to JANA2020 tools from JANADRAW is a continuing effort, as the space for improvements and additional options appears almost endless.

For modulated structures, using JANADRAW is a crucial improvement compared to JANA2006 because there are only a few programs capable of plotting modulated structures, and none of them can reflect all possibilities of JANA2020. Moreover, JANADRAW provides a so-called animation mode, in which the modulated structure is plotted in a loop as a function of the internal space coordinate t. This way, the overall structural features of the modulated structure can easily be estimated. The resulting "movies" can be saved, for instance, for later use as supplementary publication data.

We note that JANADRAW is not a tool for publication-quality figures. VESTA [16] or DIAMOND [17] are recommended for high-quality figures, and both can be called directly from JANA2020. However, for modulated structures, these programs only accept structure approximants. For the

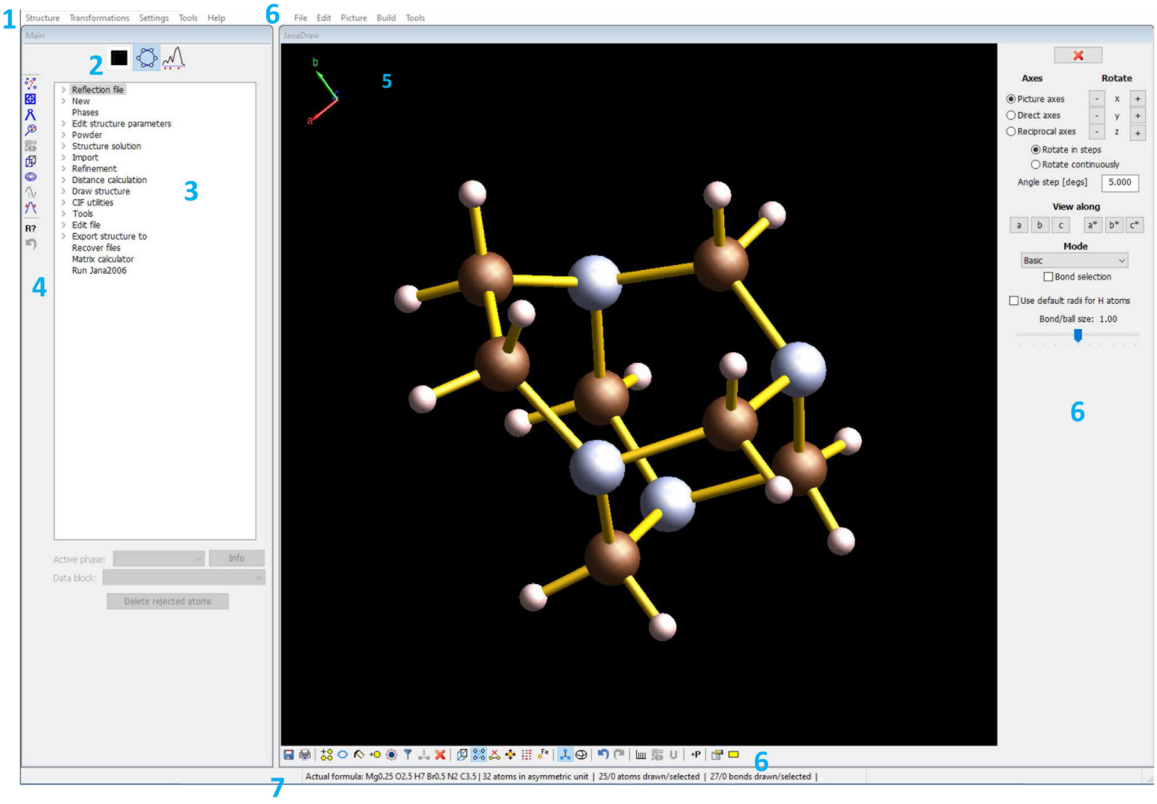

Figure 1: The user interface of JANA2020. (1) Main menu; (2) Focus buttons; (3) Command tree; (4) Quick buttons; (5) Window with the focused program – here JANADRAW; (6) program commands in the form of the menu (above), icons (below) and additional commands (right); (7) Status line with structure information summary.

introduction to the work with the graphical interface of JANA2020, we recommend the first example of the JANA2020 Cookbook – see the chapter Technical details and user support.

3 Twinning option

The article [20] describes the methods used in JANA2006 for solving and refining structures affected by twinning. Based on the type of the overlap of diffraction spots, the twins can be divided into three types for simplicity:

I. Twins by sygnonic and metric merohedry
II. Twins by reticular merohedry
III. Twins by reticular pseudo-merohedry

In the above-mentioned paper, we focused on the problem of determining the symmetry of the structure in cases where the diffraction pattern shows a higher or lower Laue group than the actual Laue group of the twinned structure. In JANA2020, the tool for determining the Laue symmetry has been improved. The program newly tests subgroups in all orientations. In addition, the user can easily include or exclude twinning resulting from the group-subgroup relations from considerations for the symmetry merging process. Considering the twin law in the symmetry merging procedure excludes those operations which do not fulfil condition (6) from Ref. [20], *i.e.*, the operations that cannot be determined directly from the diffraction pattern. We can simplify that in such a way merging of reflections across twin domains is prevented.

For example, we can choose the tetragonal structure, space group $P4_12_12$, with the Laue point group $P4/mmm$, and with the additional metric condition $c = a = b$. Then, for equally occupied domains, the Laue point group test returns results shown in Figure 2a and b, while for non-equally occupied twin domains, we obtain results shown in Figure 2c and d.

We can see that in the case of equally occupied domains, Figure 2a and b, the Laue point group test does not indicate the correct symmetry of the structure because the diffraction pattern of such crystal mimics the highest symmetry. For non-equally occupied domains, without considering twinning, the orthorhombic Laue group mmm with axes along (*c*, *a*, *b*) seems to be the correct choice. Considering the twinning, R_{int} values show that higher Laue groups are possible, and the difference between results in Figure 2c and d suggests unequally occupied twin domains. For Laue symmetry 4/*mmm*, Figure 2c, three different R_{int} values correspond to three different twin domains, and the domain with (*c*, *a*, *b*) axes is dominating as it has the lowest R_{int}. On the other hand, for Laue

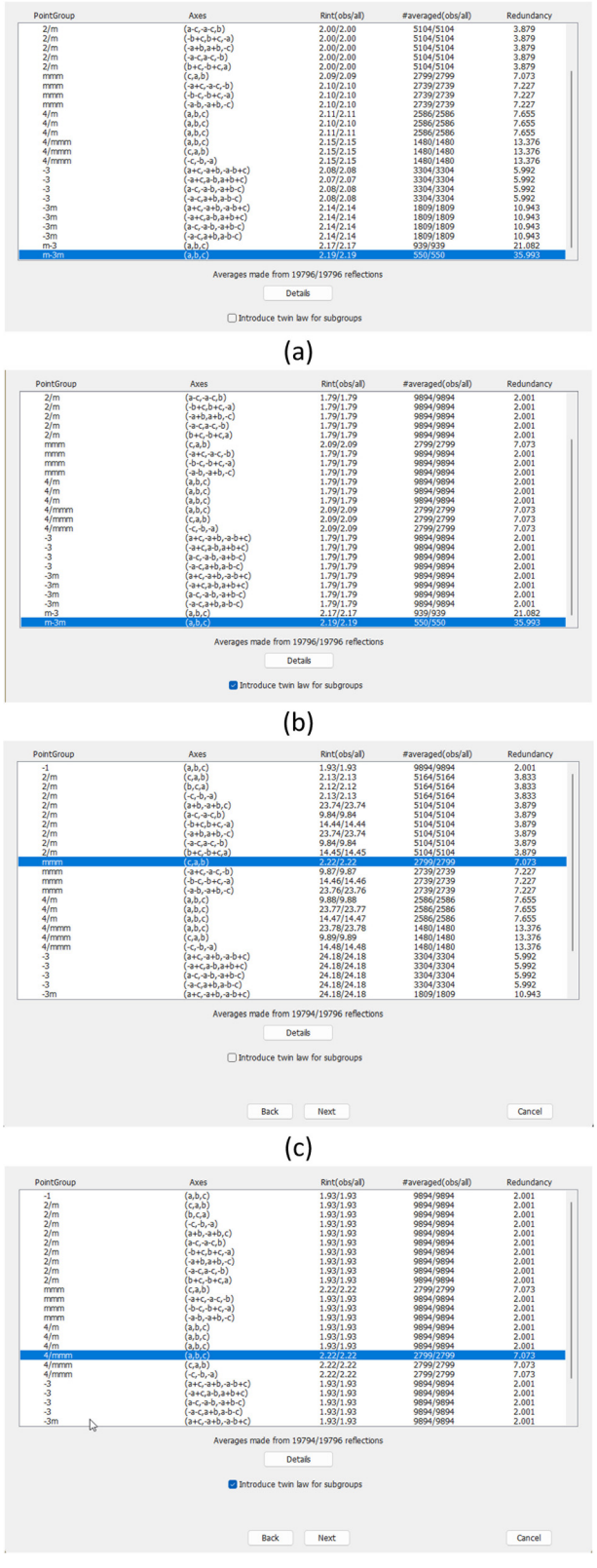

Figure 2: Results of the Laue symmetry test. (a) Equal twin domains, twinning is not considered; (b) Equal twin domains, twinning is considered; (c) Unequal twin domains, twinning is not considered; (d) Unequal twin domains, twinning is considered. The key "Introduce twin law for subgroups" causes twin laws to be considered in merging symmetry-equivalent reflections. R_{int} factors are given in %.

symmetry –3, Figure 2c shows four possibilities with the same R_{int}, which contradicts the assumption of non-equally occupied domains. Thus, the Laue symmetry 4/*mmm* with axes along (*c*, *a*, *b*) is another promising candidate for testing.

Jana2020 also helps with the structure determination of reticular twins where twinning occurs in a subcell. Due to reticular twinning, the diffraction pattern is often composed of regularly distributed clusters of diffraction spots, as it happens in the crystal of a six-fold twinned structure of β-$Ca_{11}B_2Si_4O_{22}$ (lattice symmetry 6/*mmm*, point group 2/*m*) [21]. In such a case, it is immediately evident that the pseudohexagonal unit cell, Figure 3a, found automatically by the diffractometer software, is most likely wrong.

The key to the solution is found during the unit cell centring test. Besides the standard centring vectors, Jana2020 also searches for possible non-standard centring vectors composed from halves and thirds, e.g. (1/2, 0, 0) or (1/3, 1/3, 0). For example, centring vectors found by the program are shown in Figure 4. Without considering twinning (Figure 4a), all tested centring vectors lead to many systematic absences of observed reflections. On the other hand, if twinning is considered (Figure 4b), some of the non-primitive lattice vectors having components of thirds and zeros are possible. Such diffraction pattern can be described with the three-timed smaller unit cell combined with twinning. Therefore, the user needs to confirm the possible centring vectors, and Jana2020 transforms the data to a smaller unit cell, introduces twinning, and continues with the space group test.

The newly introduced test can help recognise reticular twinning even for structures with a regular diffraction pattern. For the structure $CsLiSO_4$ used in Jana2006/Jana2020 cookbooks, the Laue symmetry test indicates an orthorhombic symmetry, but the lattice symmetry is hexagonal. The corresponding three-fold twin has an orthorhombic *C*-centred unit cell (Figure 5a). However, during the unit cell centring test, Jana2020 finds centring vectors (½, 0, 0), (0, ½, 0) and (½, ½, 0), allowing for a choice of the smaller primitive unit cell (Figure 5b), which is the correct one.

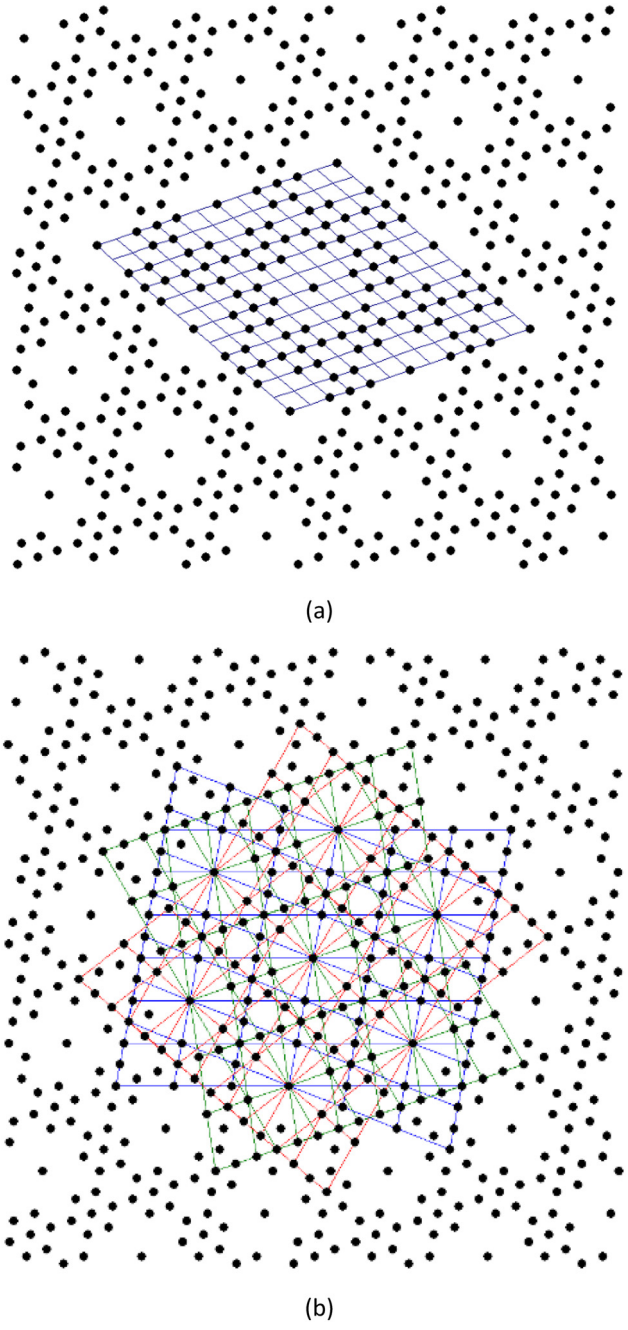

Figure 3: Simulated diffraction pattern of the six-fold twinned structure of β-$Ca_{11}B_2Si_4O_{22}$ (lattice symmetry 6/*mmm*, point group 2/*m*) published in Ref. [21]. (a) Pseudohexagonal unit cell; (b) The correct unit cell of three twin domains, related by the three-fold axis. The figure shows two triplets of existing domains. In each triplet, the unit cells are generated by the three-fold axis, shown in blue, green and red. The second triple will arise from the first triple by applying one of the remaining operations of the original hexagonal lattice point group. The diffraction patterns are simulated using the Reciprocal space viewer of Jana2020.

4 Magnetic option

The magnetic option was present in Jana2006 from 2011 and considerably improved in Jana2020. Here we briefly summarise the topic of magnetic structures and their support in Jana2020.

The arrangement of magnetic moments in the structure occurs due to the magnetic phase transition of the originally paramagnetic phase. In most cases, the nuclear structure is known from the previous structure determination, and we know the positions of individual atoms in

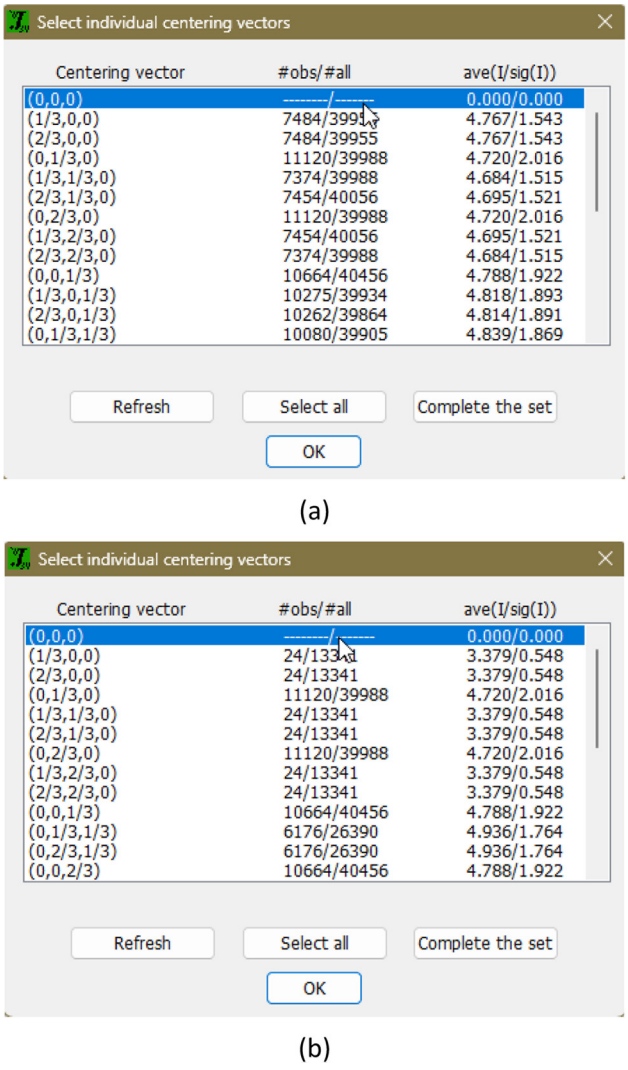

Figure 4: Centring vectors found for β-$Ca_{11}B_2Si_4O_{22}$ during the unit cell centring test. (a) Without considering twinning; (b) With considering twinning. "#obs/#all" is the number of observed/all reflections systematically absent due to the presence of the centring vector; "ave(*I*/sig(*I*))" is the corresponding average of intensity-to-sigma ratio.

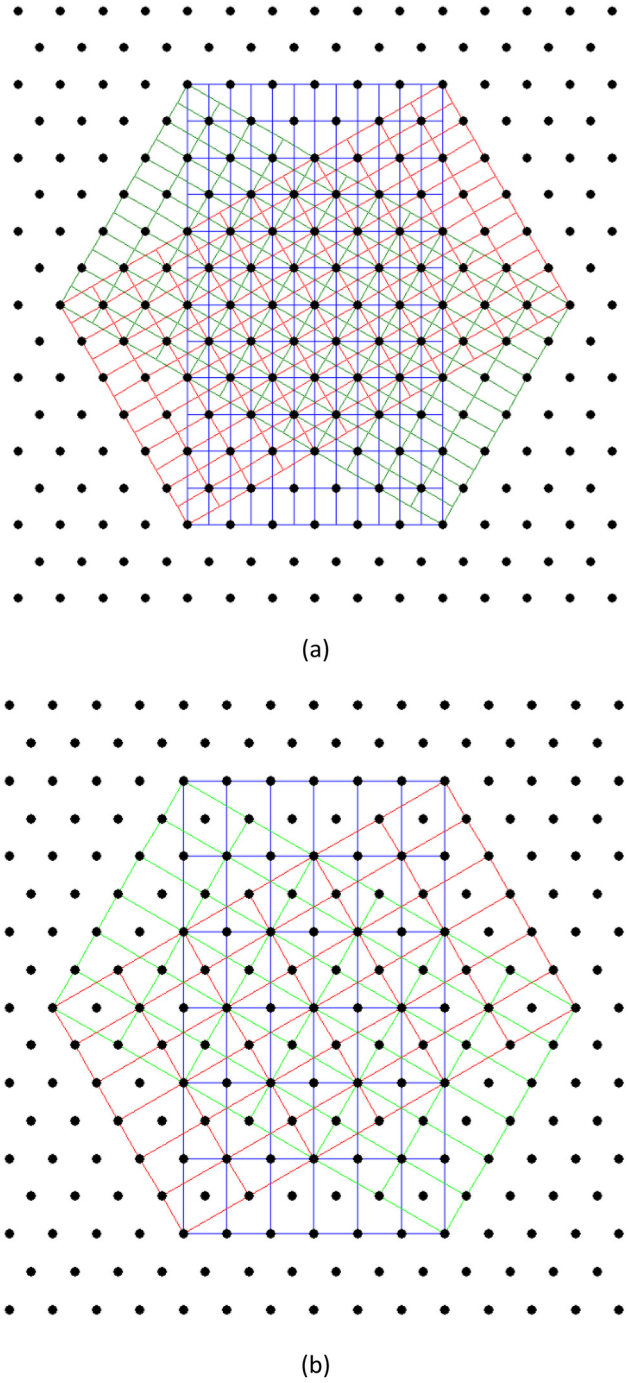

Figure 5: Two possible orthorhombic twinned unit cells in $CsLiSO_4$. (a) C-centred unit cell $\mathbf{a}_C = \mathbf{a}_H + \mathbf{b}_H$, $\mathbf{b}_C = -\mathbf{a}_H + \mathbf{b}_H$, $\mathbf{c}_C = \mathbf{c}_H$; (b) Primitive unit cell $\mathbf{a}_P = (\mathbf{a}_H + \mathbf{b}_H)/2$, $\mathbf{b}_P = (-\mathbf{a}_H + \mathbf{b}_H)/2$, $\mathbf{c}_P = \mathbf{c}_H$. "*H*", "*C*", and "*P*" indicate axes of the pseudohexagonal unit cell, C-centred orthorhombic unit cell and primitive orthorhombic unit cell, respectively. The diffraction patterns are simulated using the Reciprocal space viewer of JANA2020.

the structure and the space group. The data of this default structure is used as the so-called parent structure. The positions of atoms in the structure, however, say nothing about the arrangement of their magnetic moments.

The observed intensity of the magnetic structure sums two independent diffraction contributions: the one from the arrangement of all atoms in the structure and the other depending on the magnitude of magnetic moments of magnetic atoms [22]:

$$I(\mathbf{H}) = I_{nucl}(\mathbf{H}) + I_{mag}(\mathbf{H})$$

While the data from the diffraction experiment provide only scalar intensity, the magnetic structure factors $\mathbf{F}_{mag}(\mathbf{H})$, which play a role in the Fourier expansion coefficients of the periodic magnetisation density $\boldsymbol{\rho}_{mag}(\mathbf{r})$, are axial vectors [22]:

$$\boldsymbol{\rho}_{mag}(\mathbf{r}) = \sum_{\mathrm{H}} \mathbf{F}_{mag}(\mathbf{H}) \exp(-2\pi i \mathbf{H} \cdot \mathbf{r})$$

Moreover, the magnetic contribution, due to the use of unpolarized neutrons, is not directly proportional to the absolute value of the magnetic structure factor:

$$I_{mag}(\mathbf{H}) = \left|\mathbf{F}_{mag}(\mathbf{H})\right|^2 - \left[\mathbf{e} \cdot \mathbf{F}_{mag}(\mathbf{H})\right]^2$$

which makes a direct interpretation of Patterson or Fourier maps difficult.

The magnetic moment is an axial vector. Therefore, the even-order symmetry operations can be combined with the so-called time inversion operation. The symmetry of magnetic structures can be described with magnetic (Shubnikov) space groups [23] for cases with the propagation vector $\mathbf{k} = \mathbf{0}$ (magnetic reflections completely overlap with nuclear ones) or $\mathbf{k} \neq \mathbf{L}_n \vee 2\mathbf{k} = \mathbf{L}_m$, where $\mathbf{L}_n$ and $\mathbf{L}_m$ are lattice vectors. Magnetic superspace groups [24] are used for magnetic structures with general incommensurate propagation vectors.

Symmetry determination is considerably more complex for magnetic structures than for nuclear structures. The translational or rotational symmetry is reduced during the magnetic phase transition, and magnetic domains are formed. These usually have the same volume fractions, making the apparent symmetry of the diffraction image unchanged.

Since the magnetic structure factor has three generally independent components, three conditions must be met for the reflection to be systematically absent [25]. Therefore, analysing the diffraction picture in detail is necessary. If the magnetic atoms in the structure lie in a special position, some components of the magnetic moments may be zero or linked to each other, which can simplify the extinction conditions. For such an analysis, it is possible to use the Bilbao Crystallographic Server [26].

On the other hand, the fact that the arrangement of magnetic moments results from a magnetic phase transition allows the use of Landau's theory of phase transitions. Based on this theory, the initial paramagnetic phase is described as the magnetic type II (grey group) and decomposed into irreducible representations in representational analysis based on experimentally determined propagation vectors.

Jana2020 contains a wizard allowing users to solve magnetic structures in several successive steps described in Scheme 1. The representational analysis in Jana2020 is based on matrices of irreducible representations version 2011 as published in Ref. [27]. In the first step, an informative window (Figure 6a) shows the minimum magnetic groups associated with each irreducible representation. These subgroups are called kernels because they are composed only of operations represented by the unit matrices of the given irreducible representation [28]. In other words, their OPD (order parameter direction) has all its components non-zero and independent of each other.

The second step displays isotropic subgroups (kernels and epikernels) belonging to all irreducible representations (Figure 6b). For magnetic groups, the isotropic subgroups are arranged in blocks where the symmetry operations differ only in the position of the time inversion flag, which is combined with different symmetry operations. For magnetic superspace groups, the isotropic subgroups are arranged in blocks that differ in translational components in internal space.

After selecting a set of subgroups, we can proceed to the third step of testing and selecting models for refinement (Figure 6c). Non-zero components of magnetic moments of arbitrary size are denoted as "M", and the button "Show details" displays the complete information about symmetric restrictions. The "Global" column shows whether a given atom can contribute to ferromagnetism.

The button "Start profile simulation" compares the experimental powder profile with the calculated powder profile based on randomly chosen magnetic moments. Using this tool, in many cases, we can exclude the magnetic structure models repeatedly generating (for different random magnetic moments) observed reflections in systematically absent positions. Selected magnetic structure models can be verified by refinement running in a different instance of Jana2020, leaving the window with the parent structure available for other tests.

5 Electron diffraction

Since its introduction in 2007 [29], 3D electron diffraction (3D ED) has become a widely accepted and used tool for the structure analysis of tiny crystals [30]. Several established crystallographic programs can perform structure refinement against 3D ED data using the kinematic diffraction theory. However, the kinematical theory is a rather crude approximation. Jana2006 was the first and, with Jana2020, so far the only program that allows user-friendly structure refinement against 3D ED data using the more appropriate dynamical diffraction theory. This approach, called dynamical refinement for short, takes the dynamical diffraction effects into account and allows more accurate structure refinements [31, 32]. The dynamical refinement option is being further developed in Jana2020. Needless to say, Jana2020 also allows the standard refinement against 3D ED data using the kinematical diffraction theory.

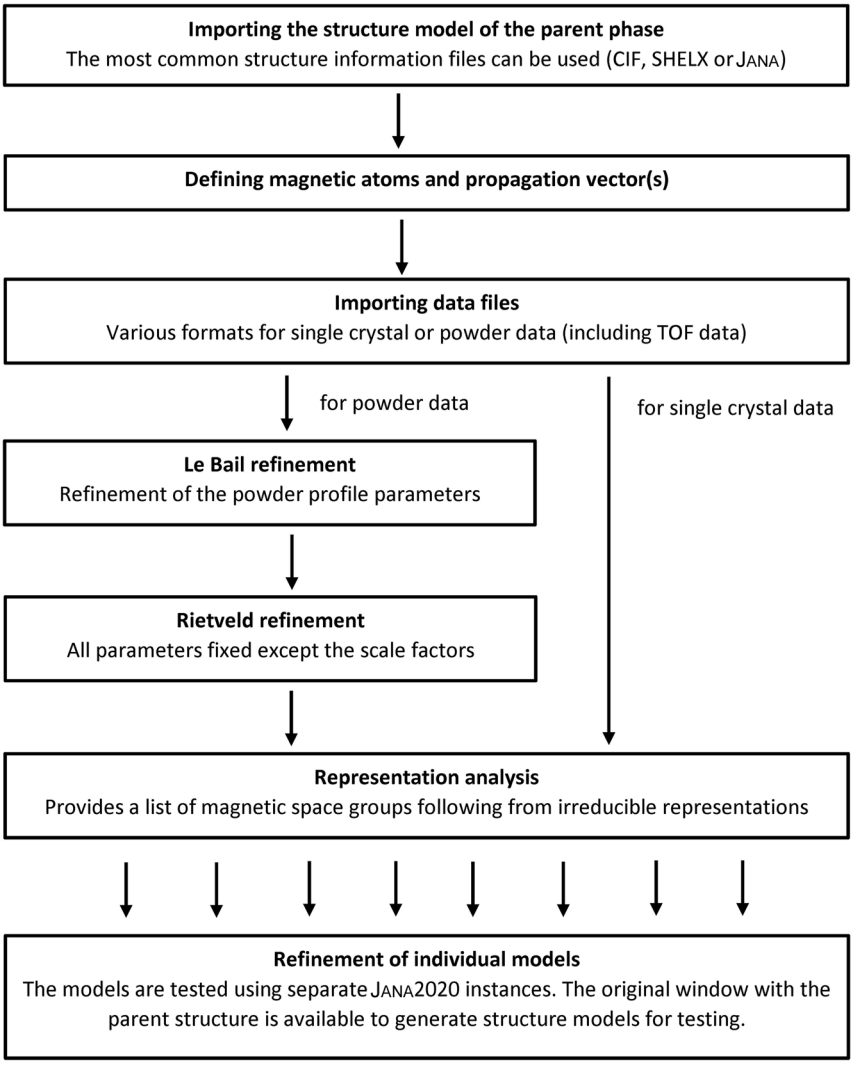

Scheme 1: Magnetic wizard of JANA2020.

Calculating dynamical diffraction intensities can be very time-consuming, and one refinement cycle may take up to several hours for large structures. Therefore, it is necessary to parallelise the calculation to speed it up. Because JANA2020 is currently not multithreaded, the computationally demanding part has been implemented in a separate auxiliary program called Dyngo. Dyngo performs the following basic tasks:

- Calculates the intensities of selected reflections based on structure factor values and calculation settings provided by JANA2020
- Calculates the derivatives of intensities with respect to the structure parameters based on the derivatives of the structure factors and other settings provided by JANA2020
- Calculates the optimal scale factor for a group of reflections recorded on a single diffraction pattern
- Finds the optimal crystal thickness for a group of reflections recorded on a single diffraction pattern

The first two tasks are usually used in the standard refinement using the dynamical diffraction theory. The procedure is seamlessly incorporated into the refinement procedure in JANA2020 and is thus entirely transparent for the user. Internally, the procedure involves steps shown in Scheme 2.

The development of this feature was continuous throughout the years. Several options have been implemented in JANA2020 that were not available in JANA2006:

- JANA2020 suggests optimal settings for dynamical refinement based on the experimental resolution, precession angle or tilt angle, and other experimental parameters
- An improved user interface is available for work with several data blocks. More data blocks are used when the

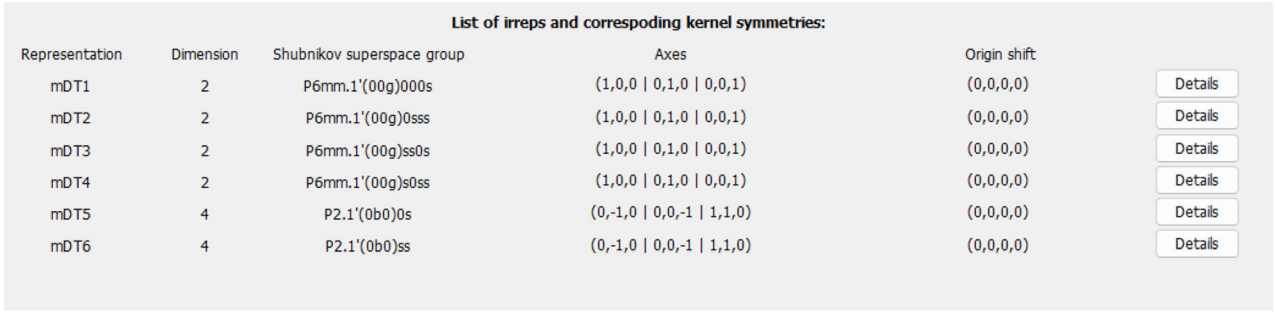

List of irreps and correspoding kernel symmetries:

Representation	Dimension	Shubnikov superspace group	Axes	Origin shift	
mDT1	2	P6mm.1'(00g)000s	(1,0,0 | 0,1,0 | 0,0,1)	(0,0,0,0)	Details
mDT2	2	P6mm.1'(00g)0sss	(1,0,0 | 0,1,0 | 0,0,1)	(0,0,0,0)	Details
mDT3	2	P6mm.1'(00g)ss0s	(1,0,0 | 0,1,0 | 0,0,1)	(0,0,0,0)	Details
mDT4	2	P6mm.1'(00g)s0ss	(1,0,0 | 0,1,0 | 0,0,1)	(0,0,0,0)	Details
mDT5	4	P2.1'(0b0)0s	(0,-1,0 | 0,0,-1 | 1,1,0)	(0,0,0,0)	Details
mDT6	4	P2.1'(0b0)ss	(0,-1,0 | 0,0,-1 | 1,1,0)	(0,0,0,0)	Details

(a)

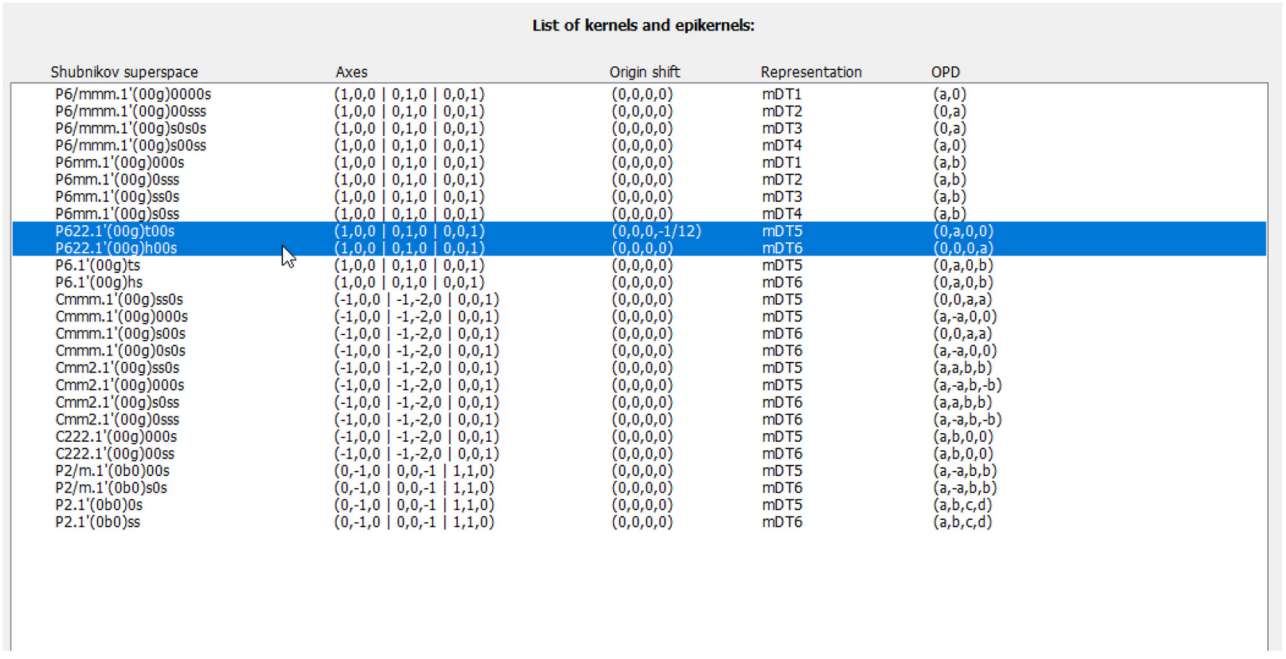

List of kernels and epikernels:

Shubnikov superspace	Axes	Origin shift	Representation	OPD
P6/mmm.1'(00g)0000s	(1,0,0 | 0,1,0 | 0,0,1)	(0,0,0,0)	mDT1	(a,0)
P6/mmm.1'(00g)00sss	(1,0,0 | 0,1,0 | 0,0,1)	(0,0,0,0)	mDT2	(0,a)
P6/mmm.1'(00g)s0s0s	(1,0,0 | 0,1,0 | 0,0,1)	(0,0,0,0)	mDT3	(0,a)
P6/mmm.1'(00g)s00ss	(1,0,0 | 0,1,0 | 0,0,1)	(0,0,0,0)	mDT4	(a,0)
P6mm.1'(00g)000s	(1,0,0 | 0,1,0 | 0,0,1)	(0,0,0,0)	mDT1	(a,b)
P6mm.1'(00g)0sss	(1,0,0 | 0,1,0 | 0,0,1)	(0,0,0,0)	mDT2	(a,b)
P6mm.1'(00g)ss0s	(1,0,0 | 0,1,0 | 0,0,1)	(0,0,0,0)	mDT3	(a,b)
P6mm.1'(00g)s0ss	(1,0,0 | 0,1,0 | 0,0,1)	(0,0,0,0)	mDT4	(a,b)
P622.1'(00g)t00s	(1,0,0 | 0,1,0 | 0,0,1)	(0,0,0,-1/12)	mDT5	(0,a,0,0)
P622.1'(00g)h00s	(1,0,0 | 0,1,0 | 0,0,1)	(0,0,0,0)	mDT6	(0,0,0,a)
P6.1'(00g)ts	(1,0,0 | 0,1,0 | 0,0,1)	(0,0,0,0)	mDT5	(0,a,0,b)
P6.1'(00g)hs	(1,0,0 | 0,1,0 | 0,0,1)	(0,0,0,0)	mDT6	(0,a,0,b)
Cmmm.1'(00g)ss0s	(-1,0,0 | -1,-2,0 | 0,0,1)	(0,0,0,0)	mDT5	(0,0,a,a)
Cmmm.1'(00g)000s	(-1,0,0 | -1,-2,0 | 0,0,1)	(0,0,0,0)	mDT5	(a,-a,0,0)
Cmmm.1'(00g)s00s	(-1,0,0 | -1,-2,0 | 0,0,1)	(0,0,0,0)	mDT6	(0,0,a,a)
Cmmm.1'(00g)0s0s	(-1,0,0 | -1,-2,0 | 0,0,1)	(0,0,0,0)	mDT6	(a,-a,0,0)
Cmm2.1'(00g)ss0s	(-1,0,0 | -1,-2,0 | 0,0,1)	(0,0,0,0)	mDT5	(a,a,b,b)
Cmm2.1'(00g)000s	(-1,0,0 | -1,-2,0 | 0,0,1)	(0,0,0,0)	mDT5	(a,-a,b,-b)
Cmm2.1'(00g)s0ss	(-1,0,0 | -1,-2,0 | 0,0,1)	(0,0,0,0)	mDT6	(a,a,b,b)
Cmm2.1'(00g)0sss	(-1,0,0 | -1,-2,0 | 0,0,1)	(0,0,0,0)	mDT6	(a,-a,b,-b)
C222.1'(00g)000s	(-1,0,0 | -1,-2,0 | 0,0,1)	(0,0,0,0)	mDT5	(a,b,0,0)
C222.1'(00g)00ss	(-1,0,0 | -1,-2,0 | 0,0,1)	(0,0,0,0)	mDT6	(a,b,0,0)
P2/m.1'(0b0)00s	(0,-1,0 | 0,0,-1 | 1,1,0)	(0,0,0,0)	mDT5	(a,-a,b,b)
P2/m.1'(0b0)s0s	(0,-1,0 | 0,0,-1 | 1,1,0)	(0,0,0,0)	mDT6	(a,-a,b,b)
P2.1'(0b0)0s	(0,-1,0 | 0,0,-1 | 1,1,0)	(0,0,0,0)	mDT5	(a,b,c,d)
P2.1'(0b0)ss	(0,-1,0 | 0,0,-1 | 1,1,0)	(0,0,0,0)	mDT6	(a,b,c,d)

(b)

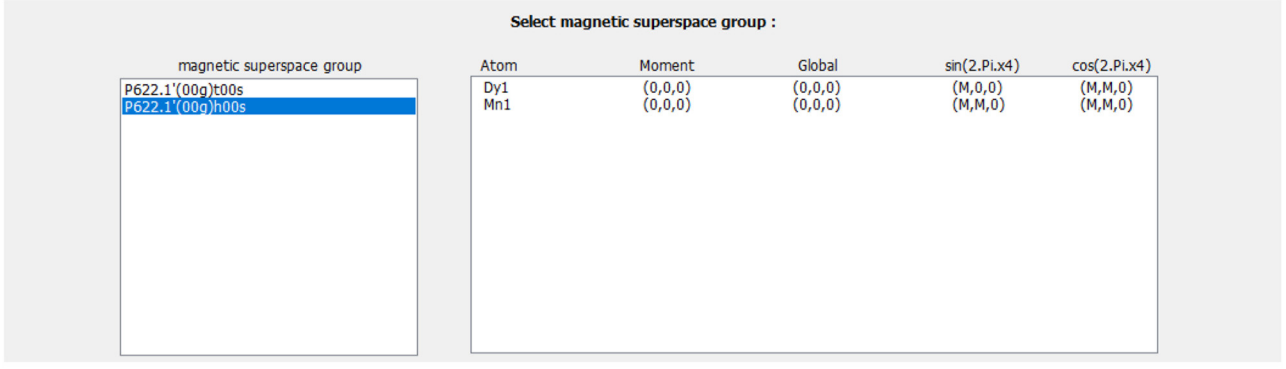

Select magnetic superspace group :

magnetic superspace group
P622.1'(00g)t00s
P622.1'(00g)h00s

Atom	Moment	Global	sin(2.Pi.x4)	cos(2.Pi.x4)
Dy1	(0,0,0)	(0,0,0)	(M,0,0)	(M,M,0)
Mn1	(0,0,0)	(0,0,0)	(M,M,0)	(M,M,0)

(c)

Figure 6: Three tools for symmetry analysis of magnetic structures. (a) Minimum magnetic groups (kernels) associated with each irreducible representation. (b) Isotropic subgroups (kernels and epikernels) related to irreducible representations. (c) Tool for testing magnetic structure models and preparing starting point for refinement.

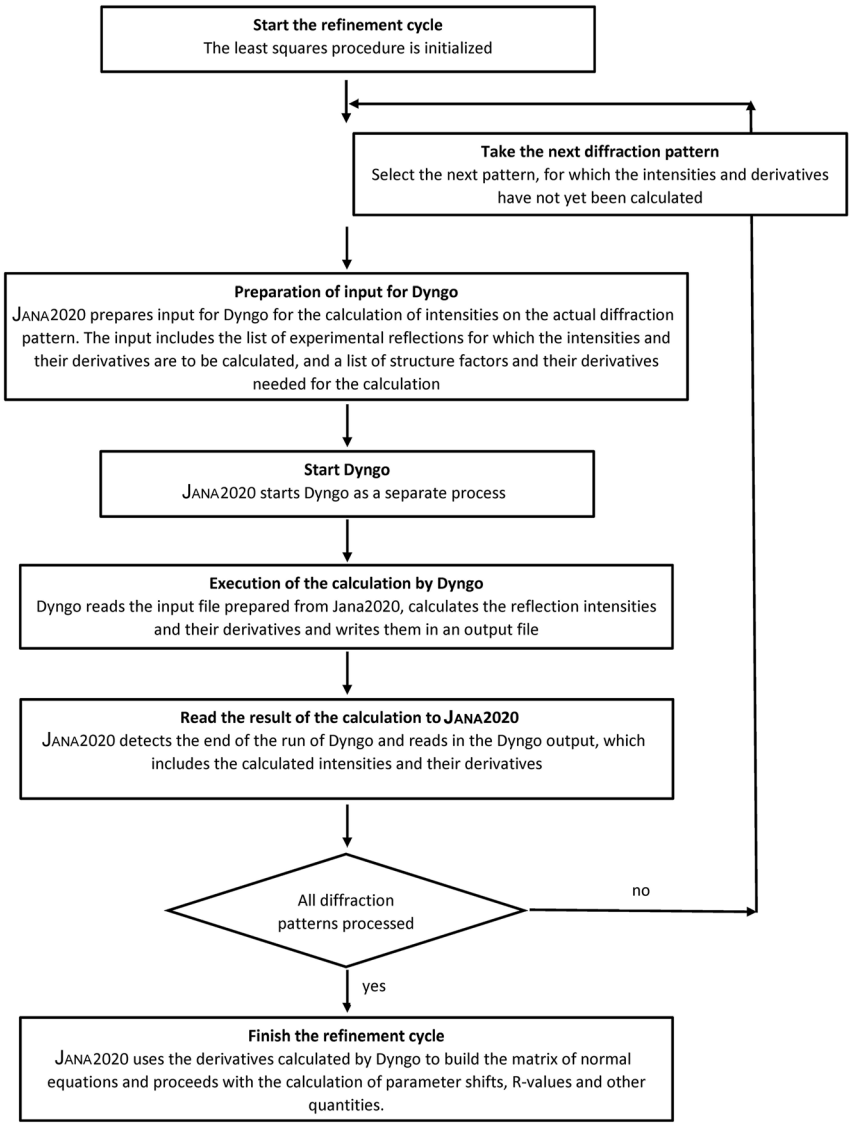

Scheme 2: Communication of Jana2020 with Dyngo.

structure is refined against data from more than one crystal.

- A 64-bit version of Dyngo is now bundled with the 64-bit version of Jana2020. This version is somewhat faster, but, more importantly, it does not suffer from the memory limitations of the 32-bit version, making it possible to deal with larger structures.
- The use of Bethe potentials [33] makes the calculation faster by a factor of more than two without a significant loss of accuracy.
- The presence of inelastic scattering can be considered in the calculation, leading to improved accuracy and more realistic estimates of crystal thickness, especially for thick organic crystals.
- It is possible to perform multipole refinement against 3D ED data. It was achieved by implementing the Mott-Bethe formula for calculating electron structure factors from X-ray structure factors, which in turn allows for direct use of the multipolar expansion of aspherical electron densities for calculating electron structure factors and their derivatives.

We will present details of the three latter features in a separate publication.

6 Special tools

Jana2020 contains several special tools out of the realm of software for structure solution and refinement. Some of them are not connected to a concrete project and, therefore, accessible from the Main menu. These tools were considerably improved in comparison with Jana2006.

The powder or single crystal data simulation simulates a data set based on the structure model. The most straightforward application is generating powder profiles from single crystal data for comparison with measured powder data. For modulated structures, we can study the influence of higher-order satellite reflections not available from the measurement on Fourier maps or powder profiles.

Cyclic refinement can be used for processing series of powder or single crystal data sets typically acquired during phase transition studies. The user defines the starting structure model and – if needed – other starting models at temperatures where significant structure model changes are expected. Jana2020 refines the structure models for remaining temperature values and visualises selected structure or profile parameters.

The indexing procedure reads peak positions obtained by peak hunting of a diffractometer software. Currently, the *tab* and *tabbin* formats of Rigaku and the *p4p* format of Bruker are supported. After reading the peak positions, the program can fully index the diffraction pattern and refine unit cell parameters, orientation matrix and modulation vectors. Although the indexing is available in commercial diffractometer software, the Jana2020 indexing procedure is sometimes helpful as an independent check, especially for twinned or modulated structures.

Absorption correction is available during data processing and offers the scaling of area detector data, absorption correction by spherical harmonic functions and absorption correction by the crystal shape. The complete correction runs with CrysAlis [34] data produced with a particular option and Bruker data, which contains direction cosines and flags indicating from which frames the reflection was integrated. Without scaling, only direction cosines are needed in the input file apart from the standard information. Similar to the indexing option, this tool duplicates the possibilities of diffractometer software and may appear superfluous. However, it can be used as an independent check, and, more importantly, because the information necessary for the corrections is included in the Jana2020 project files, absorption corrections can be repeated within Jana2020, making the tests of various options easier and faster. The corrections can also be performed even when the raw diffractometer files and related software become unavailable.

7 Jana2020 cannot …

Although Jana2020 covers most crystallographic tasks, some topics are not included. Jana2020 cannot be used for protein structures because crystallography of macromolecules uses different approaches in all steps of structure analysis, including refinement, and offering features above the possibilities of programs established in the field of protein crystallography would be highly challenging. Some proteins were found to be modulated [35], but the phenomenon is not so frequent to justify the introduction of proteins in Jana2020. For similar reasons, Jana2020 does not work with quasicrystals.

8 Technical details and user support

The Jana2020 program is written in Fortran95 and compiled by the Lahey-Fujisu and Lahey-GNU compilers [36] for the 32-bit and 64-bit versions, respectively. The graphical interface was created using the Winteracter library [3]. Jana2020 is freely available for academic users at http://jana.fzu.cz after registration. The web page links the Jana2020 Cookbook with worked examples of typical crystallographic problems resolvable with the program and announces Jana2020 workshops organised in Prague several times a year.

Acknowledgements: Jana2020 was developed within the project 18-10504S “Crystallography21” of the Czech Science Foundation. Electron diffraction methods were developed within the Czech Science Foundation project 21-05926X. Diffraction experiments used the CzechNanoLab Research Infrastructure supported by MEYS CR (LM2018110 and LM2023051).
Author contributions: All the authors have accepted responsibility for the entire content of this submitted manuscript and approved submission.
Research funding: This work was funded by Czech Science Foundation (18-10504S and 21-05926X) and MEYS CR (Czech Nanolab - LM2023051).
Conflict of interest statement: The authors declare no conflicts of interest regarding this article.

References

1. Petříček V., Dušek M., Palatinus L. Crystallographic computing system Jana2006: general features. *Z. Kristallogr.* 2014, *229*, 345–352.
2. Dolomanov O. V., Bourhis L. J., Gildea R. J., Howard J. A. K., Puschmann H. Olex2: a complete structure solution, refinement and analysis program. *J. Appl. Crystallogr.* 2009, *42*, 339–341.
3. Winteracter. The Fortran GUI toolset. Interactive Software Services Ltd. 2022. https://www.winteracter.com.

4. Petříček V., Malý K., Coppens P., Bu X., Císařová I., Frost-Jensen A. The description and analysis of composite crystals. *Acta Crystallogr.* 1991, *A47*, 210–216.
5. Palatinus L., Chapuis G. Superflip – a computer program for the solution of crystal structures by charge flipping in arbitrary dimensions. *J. Appl. Crystallogr.* 2007, *41*, 786–790.
6. Sheldrick G. Shelxt – integrated space-group and crystal-structure determination. *Acta Crystallogr.* 2015, *A71*, 3–8.
7. Burla M. C., Caliandro R., Camalli M., Carrozzini B., Cascarano G. L., Giacovazzo C., Mallamo M., Mazzone A., Polidoria G., Spagna R. Sir2011: a new package for crystal structure determination and refinement. *J. Appl. Crystallogr.* 2005, *45*, 357–361.
8. Stokes H. T., Campbel H. T., van Smaalen S. Generation of (3+d)-dimensional superspace groups for describing the symmetry of modulated crystalline structures. *Acta Crystallogr.* 2011, *A48*, 45–55.
9. Petříček V., Eigner V., Dušek V., Čejchan A. Discontinuous modulation functions and their application for analysis of modulated structures with the computing system Jana2006. *Z. Kristallogr.* 2016, *231*, 301–312.
10. Kuhs W. F. Generalised atomic displacements in crystallographic structure analysis. *Acta Crystallogr.* 1992, *A48*, 80–89.
11. van der Lee A., Boucher W. F., Evain M., Brec R. Temperature dependence of the silver distribution in $Ag_2MnP_2S_6$ by single crystal X-ray diffraction. *Z. Kristallogr.* 1993, *264*, 247–264.
12. Hansen N. K., Coppens P. Testing aspherical atom refinements on small-molecule data sets. *Acta Crystallogr.* 1978, *A34*, 909–921.
13. Cheary R. W., Coelho V. A fundamental parameters approach to X-ray line-profile fitting. *J. Appl. Crystallogr.* 1992, *25*, 109–121.
14. Dušek M., Petříček V., Wunschel M., Dinnebier M., van Smaalen S. Refinement of modulated structures against X-ray powder diffraction data with Jana2000. *J. Appl. Crystallogr.* 2001, *34*, 398–404.
15. Rohlíček J., Hušák M. Mce2005 – a new version of a program for fast interactive visualisation of electron and similar density maps optimised for small molecules. *J. Appl. Crystallogr.* 2007, *40*, 600–601.
16. Momma K., Izumi F. Vesta 3 for three-dimensional visualisation of crystal, volumetric and morphology data. *J. Appl. Crystallogr.* 2011, *44*, 1272–1276.
17. Diamond Crystal and Molecular Structure Visualization. *Crystal Impact GbR.* 2022. https://www.crystalimpact.de/diamond.
18. Macrae C. F., Sovago I., Cottrell S. J., Galek P. T. A., McCabe P., Pidcock E., Platings M., Shields G. P., Stevens J. S., Towler M., Wood P. A. Mercury 4.0: from visualization to analysis, design and prediction. *J. Appl. Crystallogr.* 2020, *53*, 226–235.
19. Hall S. R., McMahon B., Eds. *International Tables for Crystallography*; Springer: Dordrecht, The Netherlands, Vol. G, 2006.
20. Petříček V., Dušek M., Plášil J. Crystallographic computing system Jana2006: solution and refinement of twinned structures. *Z. Kristallogr.* 2016, *231*, 583–599.
21. Volkov S. N., Yukhno V. A., Bubnova R. S., Shilovskikh V. V. β-$Ca_{11}B_2Si_4O_{22}$: six-fold twinning, crystal structure and thermal expansion. *Z. Kristallogr.* 2018, *233*, 379–390.
22. Halpern O., Johnson M. H. On the magnetic scattering of neutrons. *Phys. Rev.* 1939, *55*, 898–923.
23. Belov N. V., Neronova N. V., Smirnova N. V. The 1651 Shubnikov groups. *Kristallografiya* 1957, *2*, 315–325. (English translation: Sov. Phys. Crystallogr. **2**, 311–322).
24. Janner A., Janssen T. Symmetry of incommensurate crystal phases. I. Commensurate basic structures. *Acta Crystallogr.* 1980, *A36*, 399–408.
25. Petříček V., Fuksa J., Dušek M. Magnetic space and superspace groups, representation analysis: competing or friendly concepts? *Acta Crystallogr.* 2011, *A66*, 649–655.
26. Gallego S. V., Tasci E. S., de la Flor G., Perez-Mato J. M., Aroyo M. I. Magnetic symmetry in the Bilbao Crystallographic Server: a computer program to provide systematic absences of magnetic neutron diffraction. *J. Appl. Crystallogr.* 2012, *45*, 1236–1247.
27. Stokes H. T., Campbell B. J., Cordes R. Tabulation of irreducible representations of the crystallographic space groups and their superspace extensions. *Acta Crystallogr.* 2013, *A69*, 388–395.
28. Ascher E. Permutation representations, epikernels and phase transitions. *J. Phys. C: Solid State Phys.* 1977, *10*, 1365–1377.
29. Kolb U., Gorelik T., Kuebel C., Otten M., Hubert D. Towards automated diffraction tomography: part I—data acquisition. *Ultramicroscopy* 2007, *107*, 507–513.
30. Gemmi M., Mugnaioli E., Gorelik T., Kolb U., Palatinus L., Boullay P., Hovmoller S., Abrahams J. P. 3D electron diffraction: the nanocrystallography revolution. *ACS Cent. Sci.* 2019, *5*, 1315–1329.
31. Palatinus L., Petříček V., Correa C. A. Structure refinement using precession electron diffraction tomography and dynamical diffraction: theory and implementation. *Acta Crystallogr.* 2015, *A71*, 235–244.
32. Palatinus L., Correa C. A., Steciuk G., Jacob D., Roussel P., Boullay P., Klementova P., Gemmi M., Kopeček J., Domeneghetti M. C., Camara F., Petříček F. Structure refinement using precession electron diffraction tomography and dynamical diffraction: tests on experimental data. *Acta Crystallogr.* 2015, *B71*, 740–751.
33. Bethe H. Theorie der beugung von elektronen an kristallen. *Ann. Phys.* 1928, *87*, 55–129.
34. Rigaku Oxford Diffraction. *CrysAlisPro Software System*; Rigaku Corporation: Oxford, UK.
35. Lovelace J., Petříček J., Murshudov G., Borgstahl G. E. O. Supercell refinement: a cautionary tale. *Acta Crystallogr.* 2019, *D75*, 852–860.
36. Lahey Fortran95 compiler. Lahey Computer Systems, Inc. 2022. http://www.lahey.com.

Supplementary Material: This article contains supplementary material (https://doi.org/10.1515/zkri-2023-0005).